Biochimica et Biophysica Acta 1854 (2015) 1842–1852

Contents lists available at ScienceDirect

Biochimica et Biophysica Acta

journal homepage: www.elsevier.com/locate/bbapap

Inactivation of the particulate methane monooxygenase (pMMO) in *Methylococcus capsulatus* (Bath) by acetylene☆

Minh D. Pham [a,b,c], Ya-Ping Lin [d], Quan Van Vuong [e], Penumaka Nagababu [a], Brian T.-A. Chang [a], Kok Yaoh Ng [a], Chein-Hung Chen [d], Chau-Chung Han [f], Chung-Hsuan Chen [d], Mai Suan Li [e,g], Steve S.-F. Yu [a,*], Sunney I. Chan [a,h,i,*]

[a] *Institute of Chemistry, Academia Sinica, Taipei 11529, Taiwan*
[b] *Taiwan International Graduate Program (TIGP), Academia Sinica, Taipei 11529, Taiwan*
[c] *Department of Chemistry, National Tsing Hua University, Hsinchu 30013, Taiwan*
[d] *Genomics Research Center, Academia Sinica, Taipei 11529, Taiwan*
[e] *Institute for Computational Science and Technology, Ho Chi Minh City, Vietnam*
[f] *Institute of Atomic and Molecular Sciences, Academia Sinica, Taipei 10617, Taiwan*
[g] *Institute of Physics, Polish Academy of Sciences, 02-668 Warsaw, Poland*
[h] *Department of Chemistry, National Taiwan University, Taipei 10617, Taiwan*
[i] *Division of Chemistry and Chemical Engineering, California Institute of Technology, Pasadena, CA 91125, USA*

ARTICLE INFO

Article history:
Received 16 June 2015
Received in revised form 29 July 2015
Accepted 9 August 2015
Available online 11 August 2015

Keywords:
Acetylene
Mechanism-based inactivation
Particulate methane monooxygenase
Methylococcus capsulatus (Bath)
Mass spectrometry
Computational simulation

ABSTRACT

Acetylene (HCCH) has a long history as a mechanism-based enzyme inhibitor and is considered an active-site probe of the particulate methane monooxygenase (pMMO). Here, we report how HCCH inactivates pMMO in *Methylococcus capsulatus* (Bath) by using high-resolution mass spectrometry and computational simulation. High-resolution MALDI-TOF MS of intact pMMO complexes has allowed us to confirm that the enzyme oxidizes HCCH to the ketene (C_2H_2O) intermediate, which then forms an acetylation adduct with the transmembrane PmoC subunit. LC–MS/MS analysis of the peptides derived from in-gel proteolytic digestion of the protein subunit identifies K196 of PmoC as the site of acetylation. No evidence is obtained for chemical modification of the PmoA or PmoB subunit. The inactivation of pMMO by a single adduct in the transmembrane PmoC domain is intriguing given the complexity of the structural fold of this large membrane–protein complex as well as the complicated roles played by the various metal cofactors in the enzyme catalysis. Computational studies suggest that the entry of hydrophobic substrates to, and migration of products from, the catalytic site of pMMO are controlled tightly within the transmembrane domain. Support of these conclusions is provided by parallel experiments with two related alkynes: propyne (CH_3CCH) and trifluoropropyne (CF_3CCH). Finally, we discuss the implication of these findings to the location of the catalytic site in pMMO.

1. Introduction

The pMMO is a fascinating enzyme that can efficiently oxidize straight-chain hydrocarbons from C1 to C5 with high regio-specificity and unusual stereo-selectivity [1–4]. As a membrane-bound protein, pMMO is difficult to isolate and purify to homogeneity. It is a large protein complex with three subunits, PmoA, PmoB and PmoC, and many copper ions [1,5]. Highly active protein preparations consisting of the full complement of 12–15 copper ions per protein monomer have been reported [6–9]. However, crystal structure studies from different species [10–12] have appeared showing the trimeric architecture of the pMMO complexes, each consisting of one copy of the PmoA, PmoC, and PmoC subunits, but with just 2–3 coppers and one zinc ion per monomer. This indicates a loss of some copper ions and metal replacement during the enzyme purification and crystallization [13].

Abbreviations: AMO, ammonia monooxygenase; BN-PAGE, blue native-polyacrylamide gel electrophoresis; DDM, *n*-dodecyl β-D-maltoside 98%; DHB, dihydroxybenzoic acid; EPR, electron paramagnetic resonance; FA, formic acid; GC, gas chromatography; LC, liquid chromatography; LTQFT, linear ion trap Fourier transform ion cyclotron resonance; MeCN, acetonitrile; MMO, methane monooxygenase; NADH, reduced form of nicotinamide adenine dinucleotide; pMMO, particulate MMO; MS, mass spectrometry; MALDI, matrix assisted laser desorption ionization; TOF-MS, time-of-flight mass spectrometry; SDS-PAGE, sodium dodecyl sulfate polyacrylamide gel electrophoresis; LC–MS/MS, liquid chromatography–tandem mass spectrometry; Mascot, the search engine for protein identification using MS data.

☆ This work was supported by Academia Sinica and by research grants from the National Science Council (Ministry of Science and Technology) of the Republic of China (NSC 98-2113-M-001-026; NSC 99-2119-M-001-003; NSC 100-2113-M-001-002; and 101-2113-M-001-013 to SIC; and NSC 101-2113-M-001-007-MY3 to SSFY. The computer simulations were supported by the Department of Science and Technology at Ho Chi Minh City, Vietnam and Narodowe Centrum Nauki in Poland (grant 2011/01/B/NZ1/01622 to MSL).

* Corresponding authors at: Institute of Chemistry, Academia Sinica, 128, Academia Road, Sec. 2, Nankang, Taipei 11529, Taiwan.
E-mail addresses: sfyu@gate.sinica.edu.tw (S.S.-F. Yu), sunneychan@yahoo.com (S.I. Chan).

http://dx.doi.org/10.1016/j.bbapap.2015.08.004
1570-9639/

Inconsistencies in both the number of coppers occupying the copper sites as well as the type of metal ion at the zinc site are also apparent [5].

Several models have also been proposed for the active site of pMMO as well as its overall working mechanism. On the basis of the crystal structures available, it has been suggested that the active site of the enzyme resides at the water-exposed dicopper site of PmoB (Scheme 1) [5,14]. However, based on other biophysical and biochemical studies, the site of hydrocarbon hydroxylation has been implicated to be at site D within the transmembrane domain of the X-ray structure (Scheme 1) [1,15,16]. In support of site D, a peptide–tricopper complex based on the hydrophilic peptide domain of PmoA lining this site at the interface between the PmoA and PmoC subunits has been recently prepared and shown to mediate efficient methane hydroxylation and propene epoxidation at room temperature [16]. In light of these conflicting results, the location of the catalytic site and the mechanism of methane oxidation in pMMO are still under debate [1,14,17].

Acetylene (HCCH) has long been known to be a suicide inhibitor of pMMO [18]. It has been proposed that the HCCH is oxidized to ketene (C_2H_2O) at the catalytic site and the highly reactive ketene intermediate then covalently modifies an amino acid residue in the vicinity of the hydroxylation site of the enzyme [15,18]. For this reason, HCCH is considered to be a mechanism-based probe of the enzyme catalytic site. Earlier experiments on cell extracts [18], whole cells [8], and the purified pMMO [8] using [^{14}C]-labeled HCCH as the substrate have shown that only the "~27 kDa" protein band on SDS-PAGE gels [18] is labeled with radioactivity, and N-terminal sequencing was used to assign this protein band to the PmoA subunit [8]. This observation suggests that the catalytic site of the enzyme resides within the transmembrane domain. However, there has never been any direct evidence for the oxidation of HCCH to form C_2H_2O at the catalytic site of the enzyme. It is also possible that the reactive intermediate generated by oxidation of HCCH can migrate far away from the catalytic site where it is produced in search of an appropriate target(s) for nucleophilic attack to form the chemical adduct. If so, the simple detection of [^{14}C]-radiolabeling of the pMMO subunits on a denaturing SDS-PAGE gel might lack the structural resolution to address the issue at hand.

In this study, we attempt to obtain the necessary structural data to confirm the ketene chemistry and to identify the site(s) in the protein that has been chemically modified as part of the irreversible inactivation of the enzyme. To overcome the shortcomings of the [^{14}C]-radiolabeling method, we use high-resolution mass spectrometry to identify the site(s) of the HCCH labeling of the subunit at amino-acid residue resolution. High resolution MALDI-TOF MS of the intact pMMO can be used to identify the protein subunit(s) modified and to delineate the nature of the acetylene intermediate that forms the chemical adduct with the protein. LC–MS/MS analysis of the peptides derived from in-gel proteolytic digestion of the protein subunit(s) should allow identification of the site(s) of chemical modification. In this manner, it should be possible to confirm unambiguously whether or not the enzyme oxidizes HCCH to a C_2H_2O intermediate at the catalytic site in the same manner that it hydroxylates CH_4 to CH_3OH. To assess the generality of these results, we have also undertaken parallel experiments with two related alkynes: propyne (CH_3CCH) and trifluoropropyne (CF_3CCH). Finally, computational simulation studies have been performed to gain insights into how chemical modification(s) of the pMMO subunits might inactivate the enzyme. There is presently practically no information on the interactions of small alkanes as well as alkyne substrates and their ketene derivatives in membrane proteins, not to mention their pathways of migration within the protein scaffold.

2. Materials and methods

2.1. Chemicals and materials

All chemicals for mass spectrometric analysis (dihydroxybenzoic acid (DHB), formic acid (FA), and acetonitrile (MeCN)) are ultrapure and obtained from Sigma. HCCH was obtained from Fung Ming Industrial Co., Ltd. (Taipei, http://www.fmigas.com/). CH_3CCH, CF_3CCH, *n*-dodecyl β-D-maltoside 98% (DDM) and sequencing-grade trypsin and α-chymotrypsin, were also acquired from Sigma. Blue native (BN) precast gels and running buffers were purchased from Invitrogen.

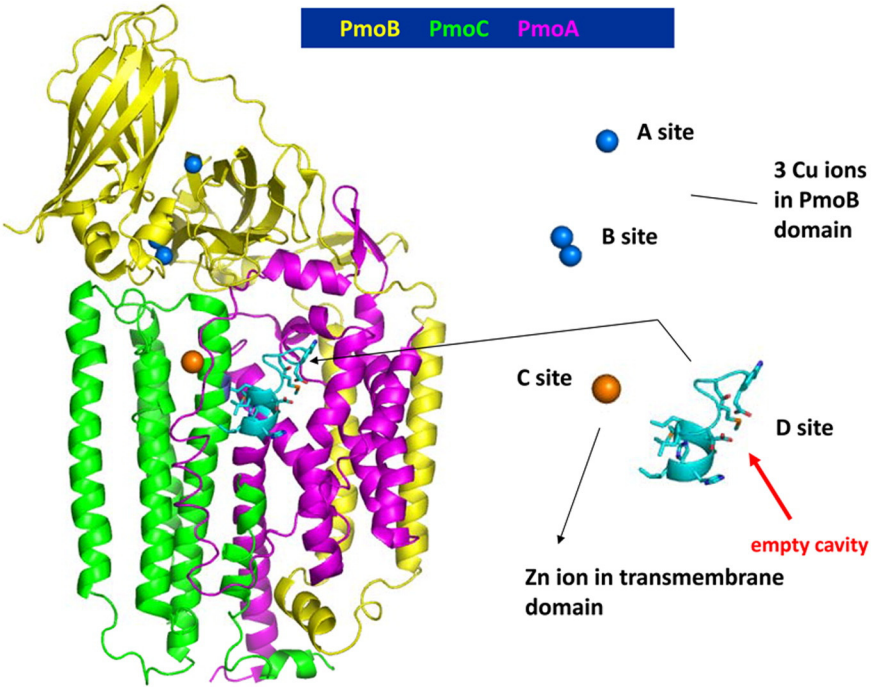

Scheme 1. X-ray crystal structure of the Cu_3-pMMO of *Methylococcus capsulatus* reported by Lieberman and Rosenzweig [10]. Ribbon diagram of the polypeptide backbones associated with the three subunits: PmoA (magenta); PmoB (yellow); PmoC (green).
Reproduced from Ref. [1].

2.2. Growth of bacteria and purification of pMMO

The growth of *Methylococcus capsulatus* (Bath) (*M. capsulatus*) strain ATCC 33009 and purification of the pMMO from the bacteria were adapted from our previous publication [7,19]. Protein samples were stored at −80 °C until use.

2.3. Kinetics of the inhibition of pMMO by HCCH, CH_3CCH, and CF_3CCH

The kinetics of the inhibition of pMMO by HCCH, CH_3CCH, and CF_3CCH were based on the whole cell assay. The propene epoxidation activity of the pMMO in the pMMO-enriched membranes of cells of *M. capsulatus* was measured at various times by GC–MS after treatment of the cells with the three different alkynes at 26 °C (a temperature lower than the optimal working temperature of the pMMO (45 °C) to reduce the rate of the inhibition reactions for easier measurements) inside a temperature-controlled incubator. In detail, *M. capsulatus* cells were prepared in 25 mM PIPES, pH 7.0, at the concentration of 0.05 g/ml. For generation of the electron donor in the cells, sodium formate was added to a final concentration of 5 mM. A slightly positive pressure in the reaction bottles was established to increase the solubility of the alkyne gas in the cell suspension by injecting 20 ml of the cell solution into a 30 ml-sealed bottle containing 15 ml of the alkyne gas and 20 ml dioxygen. Inhibition of the bacterial cells was carried out in three separate reaction bottles, one for each alkyne. The gas and the cell solution in each of these bottles were vortexed vigorously before incubation at 26 °C inside the temperature-controlled incubator. A timer was set to measure the reaction at various times: 5, 10, 20, 30, 60, and 120 min. At each designated time point, 1 ml of the cell solution was withdrawn by a syringe and added to a new sealed tube for fast vacuum removal of the suicide substrate gas before performing the propene epoxidation activity.

Assay of the epoxidation of propene was conducted in a 12 ml-sealed bottle, into which 8 ml of propene and 8 ml of dioxygen were injected by a gas syringe. The epoxidation reaction was allowed to proceed for 10 min at 45 °C. Finally, dichloromethane was added to extract the propylene oxide produced. A Hewlett-Packard HP6890 plus system equipped with a HP5873 EI–MS detector was used to measure the amounts of propylene oxide by GC–MS. Nitrobenzene was used as an internal standard.

2.4. MALDI-TOF MS

Cells treated with alkynes as described above were collected for pMMO purification. Control samples or untreated samples were also examined according to the same procedures, except that the alkyne was replaced by methane.

For the MALDI-MS of the intact pMMO complexes of the alkyne-treated samples and untreated samples, the purified pMMO protein solutions in 2% DDM were diluted to a final concentration of 0.01 μg protein/μl and 0.002% DDM by deionized H_2O, and an aliquot of the matrix solution consisting of 50 mg DHB in 70% MeCN/0.1% FA was added. Typically, 1 μl of the matrix solution was added and mixed thoroughly with the 1 μl of protein sample before application to the stainless steel plate of the mass spectrometer. MALDI-TOF-MS analysis was performed on the vacuum-dried protein crystals.

In another experiment, MALDI-MS was used in conjunction with peptide mass fingerprinting to determine the order of the PmoC and PmoA subunits in the SDS-PAGE gel of pMMO. Briefly, the two protein bands corresponding to "~27 kDa" and "~23 kDa" were first excised out of the gel of the SDS-PAGE of an untreated pMMO. In-gel digestions were performed on each of the excised protein bands with both trypsin and chymotrypsin as described in an earlier publication [20]. Sample preparation for MALDI-MS analysis of the peptides recovered from the tryptic digestion was similar to the analysis of intact pMMO.

The MALDI-TOF MS analysis of the trypsin-digested peptides and the intact protein samples were analyzed on a reflectron TOF mass spectrometer (Microflex, Bruker-Daltonics). The machine was operated in the positive ion and linear mode at an acceleration voltage of 20 kV. The laser power was adjusted to a value slightly above the desorption/ionization threshold, and the mass spectrum was obtained averaging 200 laser shots for analysis of the intact protein samples scanned across the sample surface and 100 laser shots for the digested peptides. The recorded spectrum was processed with the FlexAnalysis software (Bruker Daltonics).

2.5. LC–MS/MS

First, in order to confirm the assignment of the two lower molecular-weight bands to PmoC and PmoA in the SDS-PAGE gel by the MALDI-MS peptide mass fingerprinting described earlier, chymotryptic digests of the "~27 kDa" and "~23 kDa" protein bands in the SDS-PAGE were subjected to LC–MS/MS analysis. The use of chymotrypsin extends the sequence coverage of the mass spec analysis.

Second, LC–MS/MS analysis was used to identify the site(s) of formation of the chemical adduct(s) in the alkyne-treated samples. For the proteomic mapping of the chemical adduct(s), digested peptides were generated from both the alkyne-treated and untreated pMMO samples by the in-gel digestion method [20]. In order to obtain high protein sequence coverage, we have performed both tryptic and chymotryptic digestions of the subunits of the pMMO complex separated by BN-PAGE as well as on the three protein bands separated by SDS-PAGE. The high-resolution and high-mass-accuracy nanoflow LC–MS/MS experiments were done on a LTQFT Ultra (linear ion trap Fourier transform ion cyclotron resonance) mass spectrometer (Thermo Electron, San Jose, CA) equipped with a nano-electrospray ion source (New Objective, Inc.), an Agilent 1100 Series binary high-performance liquid chromatography pump (Agilent Technologies, Palo Alto, CA), and a Famos autosampler (LC Packings, San Francisco, CA). The digestion solution was injected (6 μl) at 10 μl/min flow rate on to a self-packed precolumn (150 μm I.D. × 20 mm, 5 μm, 100 Å), and chromatographic separation was performed on a self-packed reversed phase C18 nanocolumn (75 μm I.D. × 300 mm, 5 μm, 100 Å) using 0.1% FA in water as mobile phase A and 0.1% FA in 80% MeCN as mobile phase B operated at a 300 nl/min flow rate. Survey full-scan MS condition: mass range m/z 320–2000, resolution 100,000 at m/z 400. The ten most intense ions were sequentially isolated for MS2 by LTQ. Electrospray voltage was maintained at 1.8 kV and capillary temperature was set at 200 °C.

The raw data files acquired from the LTQFT Ultra were processed by Raw2msm (v1.10) to generate the peak lists using default parameters. The peak lists were analyzed by Mascot (v2.2.06). The search options used in this study were the user-defined database (pMMO protein sequences only), digestion enzyme trypsin or chymotrypsin, up to two or four missed cleavages, fragment ion mass tolerance of 0.6 Da and a parent ion tolerance of 10 ppm. Variable modifications were set to oxidation (M), deamidated (NQ), and carbamidomethyl (C) for control sample, C_2H_2O (HKSRC) for HCCH-treated sample, C_3H_4O (HKSRC) for the CH_3CCH-treated sample, and F_3C_3H (HKSRC) for the CF_3CCH-treated sample. Peptide ions were filtered using the cut-off score 15.

2.6. Simulation of the mass peaks in the MALDI-TOF MS

In order to quantify the level of chemical modification of the PmoC subunit in the alkyne-treated pMMO, we have de-convoluted the observed MALDI-TOF MS peak into two components corresponding to the parent and chemically modified PmoC subunits by using the peak-fitting algorithm with Gaussian function provided in the Origin 8.5 (OriginLab Corporation, USA). The Gaussian mixture decomposition of MALDI-TOF MS spectra is a widely used approach to dissect overlapping signals [21–23]. The fitting was first performed on the mass peak of the PmoC subunit derived from the untreated sample (control) in order to establish the criteria for the best fitting model, namely, the minimum number of Gaussians required to obtain optimal statistics. We found

that two Gaussian functions were sufficient to simulate the shape of the MALDI-TOF MS peak of PmoC in the pMMO of the untreated bacterial cells with a $R^2 \geq 0.95$. More importantly, the two functions have their own physical meanings, one corresponding to the parent PmoC ion (center (xc1) at m/z = 29 696, peak width at half height (w1) = 60, and curve area (A1) = 12 095) and another for the distribution of adduct ions of the PmoC with MeCN from the MALDI matrix solution (center (xc2) at m/z = 29 785, peak width at half height (w2) = 152, and curve area (A2) = 17 892). For a relative mass difference of ~90 Da between the mass peaks of PmoC and the MeCN adduct, the adduct is almost certainly the PmoC.$(MeCN)_2$ species ([M + 2MeCN + H] or [M + 83 Da]). Based on the ratio of the curve areas, the relative contribution of the two PmoC species is 1.48 in favor of the MeCN adduct.

For the HCCH- and CF_3CCH-treated samples, we have fitted the recorded MALDI-TOF MS peak of the PmoC subunit by four Gaussian functions: y = Gaussian 1 (xc1, w1, A1) + Gaussian 2 (xc2, w2, A2) + Gaussian 3 (xc3, w3, A3) + Gaussian 4 (xc4, w4, A4), where Gaussian 1 and Gaussian 2 correspond to the contributions of the unmodified PmoC and its 2:1 MeCN adduct, respectively; and Gaussian 3 and Gaussian 4 denote the contributions from the corresponding chemically modified PmoC subunit (acetylation and trifluoro-acetylenation for HCCH and CF_3CCH, respectively) and its 2:1 MeCN adduct, respectively. We assume that Gaussians 1 and 3 have the same shape, except that the latter is displaced 42 and 94 toward higher mass for the PmoC mass peaks obtained for the HCCH-treated and CF_3CCH-treated samples, respectively. The same is assumed for Gaussians 2 and 4. In other words, the mass shifts (xc3 − xc1 = xc4 − xc2) are set at 42 Da (C_2H_2O, ketene), and 94 Da (trifluoropropyne) for the HCCH- and CF_3CCH-treated samples, respectively. In addition, we used the PmoA peak as the internal standard to normalize the fitting parameters because this protein subunit does not change between samples. To obtain the best fits to the recorded PmoC mass peaks, we then vary the relative ratio between the curve areas of the chemically modified and unmodified PmoC, but maintaining the ratio of MeCN adducts A4/(A3 + A4) = A2/(A1 + A2) within the limits ~0.55–0.6. In addition, we have adjusted the width at half-height for the unmodified and chemically modified PmoC species between ~60 and ~200, namely, while keeping w1 = w3 and w2 = w4. The percentage of PmoC chemically modified during alkyne treatment of the bacterial cells is then estimated by A3/(A1 + A3) ≃ A4/(A2 + A4). For the fitting of the CH_3CCH-treated PmoC after 10 min of inhibition, two more Gaussian functions are added to the four functions to reflect the contribution of a second chemical modification of this protein subunit, and the mass shift between Gaussians 1 and 3, and between 3 and 5 (also between Gaussians 2 and 4, and between 4 and 6), is 56 Da (C_3H_4O, ketene product of propyne). The percentages of PmoC with one and two sites chemically modified are estimated by A3/(A1 + A3 + A5) ≃ A4/(A2 + A4 + A6) and A5/(A1 + A3 + A5) ≃ A6/(A2 + A4 + A6), respectively.

2.7. Docking experiments

We have used docking methods to study the interaction of O_2, the suicide substrates (HCCH and CH_3CCH) and their ketene products (C_2H_2O, C_3H_4O), CF_3CCH, as well as *n*-alkane substrates (C1–C5) and their corresponding alcohols, with the protein fold of pMMO. Crystal structures of pMMO (1YEW) [10] and (3RGB) [12] obtained from the RSCB Protein Data Bank were used for this purpose. Ions were removed and hydrogen atoms were added to the protein by the TLEAP package [24]. We used AutodockTools 1.5.4 to prepare the PDBQT file for the pMMO and ligand structures [25]. The PDBQT files were used as the input for the Autodock Vina version 1.1, which is more efficient and accurate than Autodock 4 to dock the various ligands to pMMO [26]. In Autodock Vina, the Iterated Local Search global optimizer algorithm was employed with the Shanno method [27] for local optimization. To obtain accurate results, we set the exhaustiveness equal to 1000. The maximum energy difference between the worst and best binding modes was chosen to be 7 kcal/mol. The initial positions of the ligands with fully flexible torsion degrees of freedom were generated randomly. The center of grids was placed at the center of the protein receptor. Grid dimensions were 120 × 90 × 70, which are large enough to cover the whole receptor.

3. Results

3.1. Kinetic studies of inhibition of pMMO in bacterial cells by HCCH

In principle, the inhibition experiments can be done with purified pMMO. However, it is well known that the activities of pMMO in preparations vary in the order cells > purified membrane > reconstituted protein in the detergent micelles. Moreover, earlier studies on the inhibition of pMMO by [^{14}C]-acetylene conducted on cell extracts [18], whole cells [8] or purified pMMO with good specific activity [8] gave the same labeling pattern of pMMO. For inactivation of an enzyme by a mechanism-based inhibitor, it is not possible to derive any information unless substantial portions of the proteins are active to begin with. This criterion is particularly challenging for pMMO, since not all of the proteins in pMMO-enriched membranes are active even when the bacterial cells are cultured under high copper/biomass conditions [7]. A fraction of the pMMO proteins do not contain the full complement of 12–15 copper ions to turn over hydrocarbon substrates. On the other hand, no other proteins of the cells are labeled by HCCH. For these reasons, in the present study we perform the inhibition assay with whole cells of *M. capsulatus*, in which the pMMO is overproduced up to greater than 90% of the proteins in the intracytoplasmic membranes and at least 50% of the enzymes are functional without question [7].

The results of the kinetic studies are presented in Fig. 1, where the propene epoxidation activity of whole cells is plotted as a function of the incubation time of the cells with HCCH. The propene epoxidation assay is the standard assay for determination of the pMMO activity [7, 15]. The results show that HCCH inhibits the pMMO activity totally within five to ten minutes and the inhibition is irreversible. For comparison, under similar conditions, it takes more than 2 h for the cells to consume all the reducing equivalents added to drive the turnover of the enzymes at the outset (see the line denoted "natural death" in Fig. 1). Since the activity of the whole cells remains close to 50% up to 2 h and beyond under normal circumstances, evidently the cells are still functioning until all the *active* pMMO enzymes within the cytoplasmic membranes have become inhibited by the HCCH. Thus the inhibition we observe with HCCH arises predominantly from chemical modification of the pMMO.

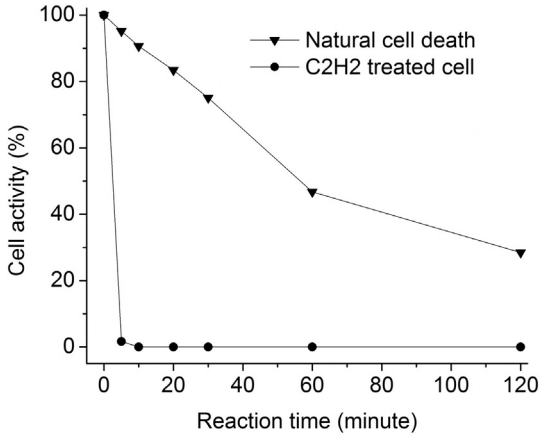

Fig. 1. Kinetics of inhibition of pMMO by HCCH based on whole cell assays. Cells of *M. capsulatus* cultured under 30 μM Cu^{2+} were treated with HCCH (C_2H_2 treated cells) at various times in comparison with the natural death of the cells. The activity of the pMMO in the cells was assayed by propene oxidation and measured by GC–MS.

Earlier studies on HCCH inhibition of pMMO have proposed that the HCCH molecule is converted to ketene at the catalytic site of the enzyme [18]. The ketene product is a very reactive intermediate, and it is thought that it readily reacts with a nucleophilic amino acid residue(s) near the active site to form a chemical adduct(s). The rate of inhibition by HCCH will depend on its rate of the penetration into the cell body to reach the intracytoplasmic membranes, the rate of diffusion of the HCCH within the cell membrane and subsequent encapsulation by a pMMO molecule, its rate of conversion into the ketene intermediate at the catalytic site of the enzyme (as it is a suicide substrate), and the rate of diffusion of the ketene intermediate within the protein to the site where the irreversible acetylation ultimately takes place. In the next section, we will address two related questions: (i) Is the HCCH indeed oxidized to the reactive ketene intermediate at the catalytic site? (ii) Where does the acetylation of the protein occur and how many turnovers are required or sufficient to inactivate the enzyme?

3.2. Identification of the pMMO subunits chemically modified by HCCH

Since there has never been any direct evidence for the oxidation of HCCH to form ketene at the catalytic site of the enzyme, we have attempted to obtain the necessary structural data to confirm the ketene chemistry and to identify the site(s) in the protein that has been chemically modified as part of the irreversible inhibition of the enzyme. To begin, we look for mass shifts (if any) in each of the three subunits after treatment with the HCCH by MALDI-TOF MS analysis of the intact pMMO complexes. The advantages of using MALDI-TOF MS are: (1) all three protein subunits in pMMO can be simultaneously analyzed in one-shot; (2) the mild conditions used to prepare the protein samples do not cause any undesired chemical-modifications of the protein; and (3) any modification(s) of the protein subunits by the acetylene inhibitor can be quantitatively analyzed with ease and good accuracy. The extreme hydrophobicity of the pMMO membrane–protein complex precludes the use of LC separation of the protein subunits for direct LC–MS analysis.

For MALDI-MS analysis, the experiment was performed at different time points in the inhibition of the bacterial cells. The results obtained for 10 min and 1 h treatments with HCCH are shown in Fig. 2 (*left panel*). (For comparison, the results for pMMO treated with CH_3CCH are depicted on the *right panel* (*vide infra*)). With the high resolution MALDI-TOF MS signals, a mass shift of 42 Da is observed clearly for the subunit with m/z 29 690 Da in the HCCH-treated pMMO sample, and the mass increment corresponds to the addition of a ketene (C_2H_2O, +42 Da) to this protein subunit. Red arrows are used to denote the development of the chemically modified species with treatment time as well as the attenuation of the signal from the unmodified spices. To confirm the mass shift, both peak fitting of the MALDI-TOF MS signal and LC–MS/MS analysis of the proteolytic peptides derived from the protein subunit were performed, as described in the following sections. The observations for HCCH-treated pMMO thus provide the first direct evidence of chemical modification of the enzyme by a ketene product.

According to the predicted masses of the three subunits of pMMO [28,29], the 29 690 Da (or 30 kDa) subunit corresponds to the PmoC subunit. Earlier suicide substrate experiments using radioactive HCCH to label the subunits, followed by SDS-PAGE, and N-terminal amino acid sequencing [8] have implicated PmoA (earlier (*vide infra*) assignment of the "~27 kDa" protein band in the SDS-PAGE gel) as the subunit labeled. Thus, our identification of PmoC as the subunit modified by HCCH is at odds with the earlier conclusion. In this study, the 30 kDa subunit has been assigned to PmoC by "high resolution" MALDI-TOF MS analysis of the intact pMMO complex without resorting to chromatography. With this method, we are able to examine the intact pMMO with the three subunits simultaneously in one direct step (Fig. S1). The observed m/z values of the three subunits are, in fact, excellently matched to their predicted masses (Table S1). Given that the PmoA and PmoC subunits are very similar in molecular mass and are not well resolved on SDS-PAGE gels, it is very likely that there is ambiguity in the assignment of the radioactivity to PmoA and PmoC. In any case, the order of the two protein subunits in the SDS-PAGE gel has been confirmed in the present study by MALDI-MS peptide mass fingerprinting of the two protein subunits (Fig. 3) as well as LC–MS/MS analysis of the in-gel proteolytic digests of the "~27 kDa" and "~23 kDa" bands excised from the SDS-PAGE gel of the pMMO complex (Fig. S2). We find that the "~27 kDa" and "~23 kDa" protein bands on the SDS-PAGE gels are PmoC and PmoA, respectively.

3.3. Quantitation of the PmoC mass shift data and correlation with the extent of inhibition of the pMMO activity

The PmoC mass signal in the MALDI-TOF MS of the pMMO protein complex is a superposition of contributions from the parent PmoC

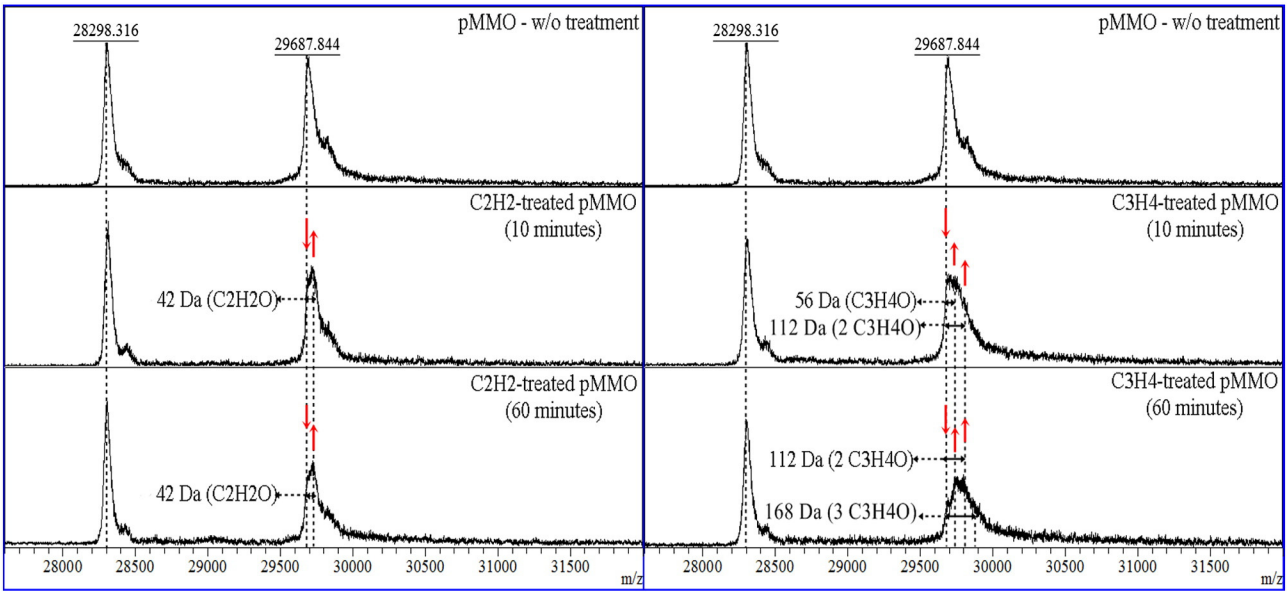

Fig. 2. MALDI-TOF MS analysis of intact pMMO treated with two suicide substrates (HCCH and CH_3CCH) in comparison with untreated samples in a time-course experiment. Whole cells were treated with and without HCCH (C_2H_2-treated pMMO) (*left panel*) and CH_3CCH (C_3H_4-treated pMMO) (*right panel*) at two time points (10 and 60 min), as described in the kinetic study (Fig. 1 and Fig. S4). Cells were then broken and the pMMO was purified. The MALDI-MS was performed directly on the intact purified pMMO proteins (see Section 2 for details).

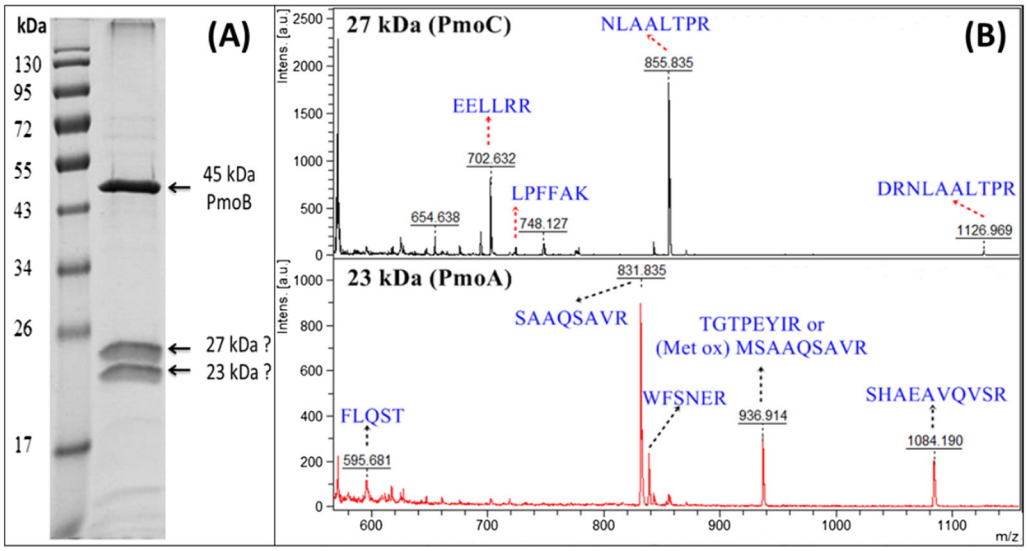

Fig. 3. The MALDI-MS peptide mass fingerprinting identification of the "~27 kDa" and "~23 kDa" protein bands excised from the SDS-PAGE gel of pMMO. Experimentally, the two bands were excised from the gel (*panel* A), and MALDI-MS analysis (*panel* B) was performed on the peptides derived from in-gel tryptic digestion as described in Section 2.

subunit plus MeCN adduct(s) of the subunit. A simulation consisting of the parent subunit (40%) and the MeCN adduct (+82 Da) (60%) is shown in Fig. 3. Upon chemical modification of PmoC by the ketene derived from HCCH, these component peaks are shifted by 42 Da toward higher masses.

Simulations of the PmoC mass peak are shown for the mass spectrum recorded after 10 min and 60 min treatment of the bacterial cells with HCCH (Fig. 4). The extent of chemical modification of the PmoC subunit (modified PmoC) upon treatment with HCCH at various time intervals could be inferred from the contribution of the remaining parent PmoC (un-modified PmoC) to the intensity at the leading edge of the composite mass signal. These results showed that about half of all the PmoC polypeptides become chemically modified by ketene in both the 10-min and 60-min HCCH-treated samples. Since the inactivation of pMMO arises prominently from HCCH treatment, this result thus suggests that only ~50% of pMMO proteins in the bacterial cells are capable of turning over and mediating oxidation of the HCCH suicide substrate to form the reactive ketene. At the level of overproduction of the pMMO protein in these bacterial cells, it would not be expected that all the pMMO residing in the membranes are active. In fact, it is known that many of these protein molecules do not contain the full complement of copper ions and the catalytic site might not even be properly assembled [7]. So, there is reasonable correspondence between the level of chemical modification of the PmoC subunit deduced from analysis of the mass signal and the extent of inhibition of the pMMO enzyme in the bacterial cells. Both sets of data showed that the inhibition of the cells by HCCH is complete within 10 min.

Analysis of the PmoC mass signal also indicates that the acetylated subunit arises from the reaction of PmoC with only one ketene molecule. As there is no significant change in the mass peak between 10 and 60 min, we surmise that it takes the modification of one site to inactivate the enzyme, and the rate of chemical modification is very rapid. The rapid acetylation suggests that the ketene has reacted with an amino acid residue at or close to the catalytic site where the HCCH is oxidized, or the ketene has migrated rapidly within the product exit channel away from the catalytic site to the location where the chemical modification has finally taken place. To distinguish between the two possibilities, we will identify the site of formation of the chemical adduct by bottom-up proteomics as described in the next section.

Thus, on the basis of the MALDI-TOF MS analysis, we have obtained direct evidence that HCCH is first converted into ketene by the catalytic site of pMMO and the reactive intermediate then chemically modifies *one* amino acid residue of PmoC subunit, but not PmoA, leading to the enzymatic inactivation. Due to lower resolution of MALDI-TOF MS at higher masses, we could not determine a clear mass shift of PmoB, the largest of the three subunits (Fig. S1, *right panel*). In any case, [^{14}C]-acetylene labeling experiments reveal no chemical modification of the PmoB subunit [18].

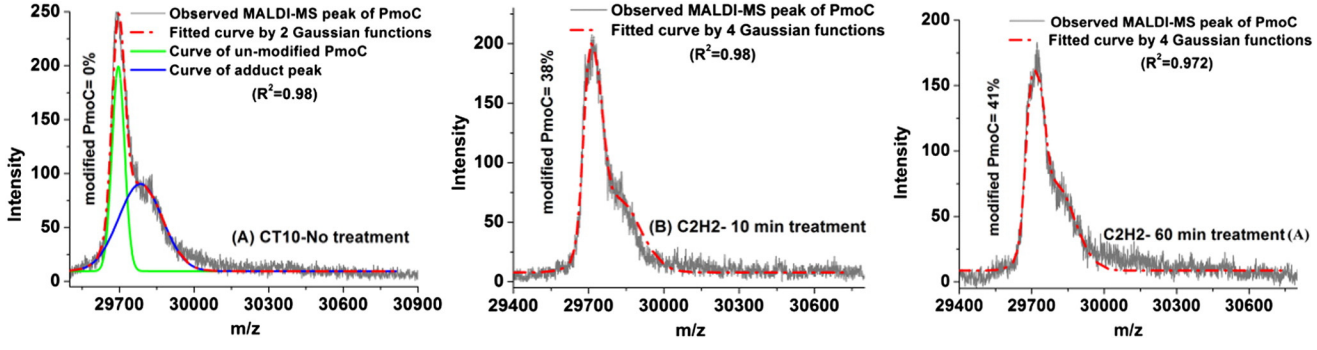

Fig. 4. Quantitation of the PmoC mass shift data. Fitting of the mass signals of the PmoC subunit from untreated and HCCH-treated pMMO (C_2H_2-treatment) to a sum of contributions from chemically modified and unmodified species. The percentage of chemically modified PmoC subunit was determined from the relative contribution of the two species to the composite PmoC mass signal in each case: *panel* A, untreated pMMO; *panel* B, C_2H_2-treated pMMO (10 min); and (*panel* C), C_2H_2-treated pMMO (60 min). Two Gaussian functions and four Gaussian functions were used to fit the unmodified PmoC subunit and HCCH-modified PmoC subunit, respectively. For details of the fitting, see Section 2.

3.4. Identification of the site(s) of chemical modification leading to the irreversible inactivation

To obtain structural data on the site of chemical modification by HCCH at higher spatial resolution, we have analyzed the peptides generated by in-gel proteolytic digestions of the chemically modified subunit of the HCCH-treated pMMO samples by LC–MS/MS. First, the results of this "bottom-up" proteomics study on the pMMO subunits offer confirmation of the conclusions derived earlier from the MALDI-TOF MS analysis. The MS/MS analysis identifies *one* peptide (YAKTRLPFF) that has been modified by the oxidation product of HCCH based on mass shifts: ketene (C_2H_2O), a mass shift of +42.0106 Da. In addition, the ketene has formed a chemical adduct with residue K196 in the PmoC subunit. So, the present proteomics analysis confirms our earlier deduction from the MALDI-MS experiments that the pMMO activity is totally inhibited by chemical modification at a single site (K196) in the PmoC subunit by ketene. Evidently, it takes only one turnover of the enzyme and the acetylation of one site in the protein to inhibit the activity. Interestingly, the residue modified is quite far away from either the PmoB dicopper site in the water-exposed domain or the putative tricopper site embedded within the membrane. Thus, the ketene produced at the catalytic site upon oxidation of HCCH must have migrated away from the catalytic site to form a chemical adduct with an amino acid along some specific substrate-product channel(s).

With the peptide sequencing of the inhibited pMMO samples by multiple LC–MS/MS runs, only 70% sequence coverage is obtained with the peptide sequencing of PmoA and PmoC (Fig. S3). However, all potential amino acid residues (lysines, histidines) in the vicinity of the putative tricopper site available for chemical modification by ketene have been identified by the peptide sequencing method. The sequences of PmoA and PmoC that are not covered in the peptide sequencing are associated with the hydrophobic α-helices that line the peripheral boundary of the three-dimensional structure. In any case, our peptide sequencing data are consistent with the MALDI-MS results. For the PmoB subunit, we have obtained more than 90% sequence coverage (Fig. S3). This extensive coverage has allowed us to examine almost the entire PmoB subunit for amino acid residues that might be chemically modified (if any). Importantly, all amino acid residues residing within the vicinity of the dicopper site have been covered in the present study.

3.5. Inhibition of pMMO by CH_3CCH and CF_3CCH

The pMMO is also inhibited by CH_3CCH and CF_3CCH. As expected, CH_3CCH behaves like HCCH, namely, it is first oxidized to methyl ketene, which then acetylates the PmoC subunit. However, the kinetics of inhibition is significantly slower, and we observe multiple acetylations of the protein subunits with time. The inhibition by CF_3CCH is even slower. With this inhibitor, there is no evidence that oxidation is involved, so it is evidently not a suicide substrate.

3.5.1. CH_3CCH

The kinetics of inhibition of the pMMO activity of whole cells by CH_3CCH is presented in Fig. S4. Whereas HCCH inhibits the propene epoxidation totally within five minutes, it takes 30 min in the case of CH_3CCH to completely inhibit the same amount of cells under otherwise identical conditions. MALDI-TOF MS analysis of the intact pMMO complexes at time points of 10 min and 1 h of inhibition of the bacterial cells are shown in Fig. 2 (*right panel*). Again, a mass shift is observed only for the PmoC subunit. Simulation of the PmoC mass peak recorded at 10 min yields an increment of 56 Da for the CH_3CCH-treated cells (Fig. 2 and Fig. S5). This mass increment corresponds to the addition of methyl ketene, CH_3CCHO (+56 Da) to this protein subunit. Interestingly, the width of the observed PmoC mass spectrum increases with time (Fig. 2 and Fig. S5), indicating that there is multiple modifications of this protein subunit with this inhibitor. More than one protein sites can be acetylated if additional propyne substrates can be oxidized by a given pMMO enzyme before it is eventually inhibited by a methyl ketene. Such a scenario is possible with a bulkier suicide substrate like propyne. The methyl ketene is expected to migrate more slowly away from the catalytic site where it is formed. This ketene derivative is also intrinsically less reactive compared with ketene [28,29]. Consistent with the results noted earlier for HCCH-treatment, simulation of the PmoC mass peak of the CH_3CCH-treated pMMO after the 1-h reaction shows that ~50% of the PmoC subunits in the sample are chemically modified when the pMMO activity has become completely inhibited (Fig. S5). Thus this result also indicates that *ca*. 50% of the pMMO in the membranes of the bacterial cells are sufficiently active to convert CH_3CCH into its ketene intermediate.

LC–MS/MS analysis identifies peptides that have been modified by methyl ketene based on the mass shift of +56.0262 Da (Table S2). The acetylation occurs primarily at residue K196 (PmoC), the same lysine that is acetylated by ketene for inhibition by HCCH. The methyl ketene also modifies K48/K49 and S277 (PmoC), supporting the multi-modifications of the PmoC subunit with this inhibitor.

3.5.2. CF_3CCH

It takes almost an hour for CF_3CCH to completely inhibit the pMMO activity of the bacterial cells under otherwise identical conditions (Fig. S4). MALDI-TOF MS analysis of the intact pMMO complexes at time points of 10 min and 1 h into the inhibition of the bacterial cells are shown in Fig. S6. Again, a mass shift is observed only for the PmoC subunit. Simulation of the PmoC mass peak recorded at 10 min yields an increment of 94 Da for the CF_3CCH-treated cells (Fig. S7). This mass increment corresponds to the addition of CF_3CCH (+94 Da) to this protein subunit. Apparently, CF_3CCH reacts with pMMO by direct addition to an amino acid residue rather than a mechanism that involves a ketene product of the trifluoropropyne substrate. As in the case of HCCH, it takes the modification of one site on the PmoC subunit to inactivate the enzyme, although the rate of inhibition is significantly slower. LC–MS/MS analysis identifies one peptide from the PmoC subunit with a mass shift +94.003 Da, and it is C279 (PmoC) that is trifluoroacetylenated (Table S2). Since CF_3CCH directly forms a chemical adduct with an amino acid and inactivates the enzyme without prior oxidation at the catalytic site, it is not a substrate-based inhibitor but merely an irreversible inhibitor. Analysis of the PmoC mass signal reveals that only 36% of the pMMO proteins are irreversibly modified after 60 min of the treatment. CF_3CCH not being a suicide substrate, we would have expected the PmoC subunits in the bulk of the pMMO in the cells to be chemically modified.

3.6. Docking acetylene, n-alkane substrates and their oxidation products, and dioxygen to the three-dimensional structure of pMMO

Crystal structures of pMMO, so far, have not provided any direct evidence for substrate or product binding site(s) and migration pathway(s) of substrates/products within the protein fold. This is hardly surprising, as substrate and product channel(s) are dynamic, not static, and are more likely created by interactions of the substrate/product during migration to and from the catalytic site. Information of this kind has been obtained for some enzymes by growing protein crystals in the presence of xenon gas to mimic the trapping of substrates or products formed at the catalytic site [30–32]. A xenon atom, despite its size and polarizability, is hardly representative of a hydrocarbon substrate, except perhaps for methane, but certainly not propene and HCCH, not to mention methanol, ketene, and propylene oxide. To move forward, we use computer simulations to dock various substrates and products relevant to the present study, including HCCH, CH_3CCH, *n*-alkane substrates and their oxidation products, to pMMO using the protein folds offered by the crystal structures of the enzyme as a point of departure. The identification of K196 in PmoC provides at least one data point for us to check the validity of the approach. There must be a binding pocket for the

product ketene and methyl ketene in this region of the transmembrane domain to allow it to covalently modify this lysine side chain during the formation of acetylated adduct. Elsewhere in the protein, there must be also binding sites for methanol, the product of the methane oxidation, near the membrane-aqueous interface on the cytosolic surface, since methanol dehydrogenase, the next enzyme in the C1 metabolic pathway of the organism, is known to bind to pMMO in this region [33]. Thus, although the X-ray crystal structures of pMMO do not contain the full complement of metal cofactors as in the active enzyme embedded within the lipid bilayer, the availability of these structures can still offer the opportunity to identify potential substrate-binding sites in the transmembrane domain by computer docking experiments [34,35]. However, it is important to point out here that while the docking experiments are sufficiently accurate to locate the binding sites of small molecules in the protein fold as determined by the X-ray structure, the results pertain only to the "static" fold of the enzyme in its "native" structure. The docking method does not, and cannot, address the dynamics of the protein system. We need to simulate these protein fluctuations before the details of the transport or migration of a given substrate or product molecule from one binding site to another within the protein fold can be captured. Computational simulations of protein dynamics are beyond the scope of this study.

The predicted binding positions for HCCH and its ketene intermediate are shown in Fig. 5. It is noted that K196 of PmoC is in close proximity with three affinity positions (**P1**, **P2**, and **P3**), all within the same region of the alpha-helix bundle of PmoC and at the interface between the PmoC and PmoA subunits near the periplasmic face of the transmembrane domain. A ketene residing at **P1** would be only several angströms away from this lysine. Interestingly, the **P1** position also has the highest affinity for ketene compared to the other binding sites in the enzyme. Another position (**P2**), which is closest to the K196 residue, shows the second highest binding affinity toward ketene. There is only one other HCCH or ketene binding site (**P4**) predicted in the transmembrane region, and two others (**P5** and **P6**) in the water-exposed domain of the PmoB subunit, but these sites are far removed from potential lysine residues to facilitate nucleophilic attack by the reactive ketene. Thus, it seems that the formation of the chemical adduct at K196 is perhaps not an accident, as there is a thermodynamic driving force for a ketene formed at the catalytic site to find its way to this region of the protein for the acetylation reaction. We have compared the results of docking experiments between the two crystal structures of pMMO available [10,12] and the same outcomes are obtained (Fig. 5 and Fig. S8).

In order to understand how acetylation of K196 of PmoC can abolish the activity of a big protein complex like pMMO, we have performed similar docking studies with hydrocarbon substrates of pMMO (C1 to C5) and their corresponding product alcohols. The results obtained reveal that all the *n*-alkanes share the same binding locations as HCCH and CH_3CCH (Fig. S9). Thus, there must be some overlap in the pathway(s) of entry of all these substrates into the protein. In addition, they all dock into the cavity close to the putative tricopper site (site D) of the enzyme [34]. Thus, it would seem that the pMMO uses the same substrate pathway(s) to deliver hydrocarbon substrates including the suicide substrate HCCH to the active site of the enzyme. Importantly, all *n*-alkane substrates of pMMO and their alcohol products as well as HCCH all have the same affinity binding sites at **P1**, **P2**, and **P3** as for ketene. Since the ketene adduct of K196 in this domain of the protein totally abolishes the pMMO activity, the chemical modification very likely has disrupted the substrate/product pathway(s) to the active site of the enzyme. Interestingly, K196 is embedded within a highly disordered region of the protein structure in the lipid bilayer nearby C279 (PmoC), where one modification of CF_3CCH also can abolish the enzyme activity. For comparison, none of the hydrocarbon substrates of pMMO as well as HCCH shows affinity near the dicopper site (site B) in PmoB, or the zinc site (site C) in PmoC, of the X-ray structure.

Similar docking of the product alcohols of the pMMO hydrocarbon substrates reveals six additional binding sites (Fig. S10). The binding affinity varies with the product alcohols, and as expected, there are more binding sites for the alcohols than for the parent hydrocarbons in the cavity of the putative tricopper site. This latter result underscores the importance of product release from the active site in controlling the catalytic cycle of the enzyme.

We have also studied the binding of O_2 to pMMO. These docking experiments have resulted in some interesting findings (Fig. S11). Generally speaking, the O_2 molecule tends to have very good affinity for the

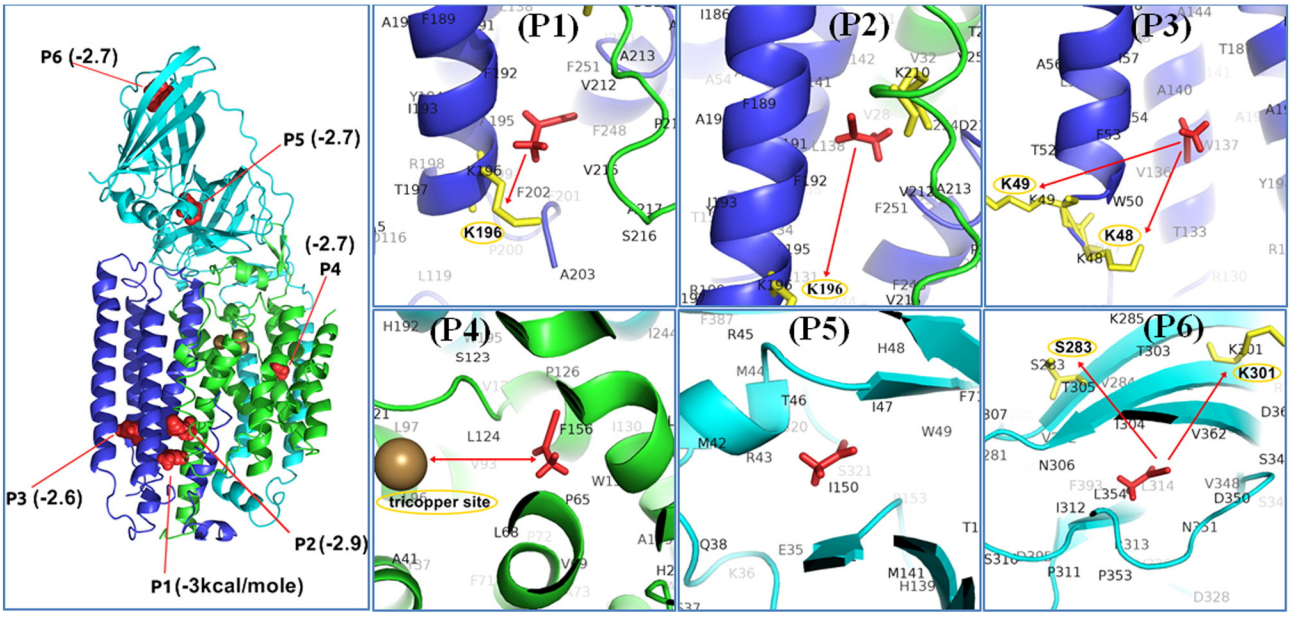

Fig. 5. Molecular docking of ketene and HCCH to pMMO. The representative molecule in red is ketene, which has binding affinity to all six positions from **P1** to **P6**. Predicted binding energy (kcal/mol) of ketene to each position is provided in parentheses showing the highest binding affinity for **P1** and **P2**. HCCH has five affinity-binding sites (**P1** to **P4** and **P6**), but no binding affinity for **P5** (the corresponding binding energies are provided in Fig S9). The surrounding residues of the four ketene affinity sites within the transmembrane domain are also presented in the right. K196 is underscored in (**P1**) showing its proximity to the affinity binding site number **1** or **P1**, which is also within the cluster of the two other sites **P2** and **P3**. The putative tricopper cluster (D site) is highlighted in brown spheres. Crystal structure of pMMO from *M. capsulatus* used in this study is reproduced from PDB (accession number 1YEW). Similar results are also obtained for molecular dockings performed on the revised crystal structure of pMMO (Fig. S8).

water-exposed "soluble" domain of the protein. Only a few binding sites are located within the transmembrane domain, but two reside within the cavity of the putative tricopper cluster (site D). The implication is that O_2 approaches the active site of pMMO from the water-exposed protein domain on the cytosolic side of the membrane and diffuses to site D for activation of the tricopper cluster.

4. Discussion

In this work, we have studied the inactivation of pMMO embedded in the membranes of *M. capsulatus* by HCCH using high-resolution mass spectrometry and computational simulations. The results have allowed us to confirm that HCCH is indeed a mechanism-based inhibitor of the enzyme [18]. It is first oxidized at the catalytic site to ketene, which then migrates within the product exit/release channel(s) of the enzyme to form a unique chemical adduct with K196 of PmoC in the transmembrane domain near the periplasmic surface. Significantly, this chemical modification alone by ketene can disable the substrate entry channel(s) and irreversibly inhibit the enzyme.

Earlier workers have used [^{14}C]-labeled HCCH as the mechanism probe of the catalytic site and have detected the radioactivity primarily in the "~27 kDa" subunit in denaturing SDS-PAGE gels of the protein [8, 18]. In the latter work [8], the labeling experiment is not clean, leading to the observation of [^{14}C]-radioactivity in the protein band corresponding to the PmoB subunit as well as other cytoplasmic proteins (Fig. 3 of ref 18). Subsequently, the "~27 kDa" subunit was assigned to PmoA by N-terminal sequencing [8]. Accordingly, there has been general consensus that the active site of the enzyme is associated with the PmoA subunit (not PmoB as mentioned in [14]). In the present study, however, we find only evidence for chemical modification of the PmoC subunit by ketene in the MALDI-TOF MS and LC–MS/MS experiments. No mass shift is observed for PmoA. Thus, it appears that these mass spec results are in conflict with the earlier radiolabeling experiments. However, since we confirm that the "~27 kDa", and "~23 kDa" protein bands in SDS-PAGE gel are PmoC and PmoA, respectively, by MALDI-MS mass-finger printing (Fig. 3) as well as LC–MS/MS based subunit-protein identification (Fig. S2), the assignment of the PmoC and PmoA bands in the SDS-PAGE gels appears to have been reversed in the earlier studies. In light of this, our present MALDI-MS results are actually in agreement with the radiolabeling experiments. Proteomics analysis of the peptides derived from in-gel proteolytic digestion of the subunits from the chemically modified pMMO complexes show that it is K196 of the PmoC subunit that is acetylated, providing further evidence that it is PmoC, not the PmoA subunit, that is being modified.

It is significant that it takes only the acetylation of one site (K196, PmoC) for HCCH (and CH_3CCH as well) to inactivate the pMMO. According to the crystal structure, the distance from this lysine to the putative tricopper site is ~42 Å, and the corresponding distance to the PmoB dicopper site is ~58 Å. This observation suggests that ketene has migrated rapidly within the product exit channel away from the enzyme catalytic site to the location where the acetylation has finally taken place. With this scenario, the catalytic site should remain intact after acetylation of PmoC by ketene. Indeed, it can still be activated by O_2, and it is still possible to transfer reducing equivalents from NADH to the site to turn over dioxygen [15,36]. Evidently, the inactivation of the enzyme inhibits only the hydroxylation/epoxidation of hydrocarbons, but not oxidase chemistry. Thus, the inactivation of the enzyme upon acetylation of PmoC probably arises from blockage of a unique gate for entry of the natural alkane substrates into a channel that leads to the enzyme active site. It could be also that this chemical modification inhibits the formation of a substrate channel elsewhere in the transmembrane domain by suppressing the protein dynamics or conformational fluctuations required for creation of such a pathway to allow substrates to reach the catalytic site. Given that the affinity binding sites of HCCH, ketene, methyl ketene, and hydrocarbon substrates of the enzyme at **P1**, **P2**, and **P3** are close to one another, and the binding pockets might even overlap to some degree according to the docking simulations, the distinction between the two scenarios on how acetylation of K196 (PmoC) might interfere with the formation of substrate entry pathways borders on semantics. In any case, these channels are not to be construed as fixed or static channels, and are accordingly not seen in the X-ray crystal structures of the protein. Rather, they are dynamic channels, nucleating by penetration of a substrate into the protein structure or formation of a product molecule, and created by propagation of the substrate or product molecule throughout the structure by excitation of the protein dynamics.

It is interesting that acetylation of one amino acid at a single site as distant as 40–60 Å away from the catalytic site can efficiently inactivate the hydrocarbon oxidation activity of the enzyme. Thus, access of substrate molecules to the catalytic site of the enzyme must be controlled tightly within the alpha-helical bundle spanning the membrane. This single observation alone has led us to conclude that the catalytic site of the enzyme must be sequestered within the transmembrane domain of the protein in a pocket or region well protected by surrounding hydrophobic amino acid residues of the helix bundle. The implication is that the catalytic site of the enzyme must not be located in a water-exposed domain, such as the PmoB dicopper site. Examination of the X-ray crystal structure of the pMMO indicates that the region of the protein containing the PmoB dicopper site is hydrophilic and solvent-accessible (Fig. 6). In addition, there is no hydrophobic channel(s) connecting the dicopper site to the site of acetylation within the transmembrane domain. Thus, if the ketene were indeed formed by oxidation of HCCH at the dicopper site, this reactive intermediate would rapidly react with water in the aqueous buffer to give HCOOH, and with O_2 to give CO_2 and HCHO [29,37].

Within the transmembrane domain, there is one "zinc site" observed in the crystal structures [10–12] and the putative tricopper site that is proposed to be located at site D of the protein [1,16]. A dioxo-diiron cluster has also been suggested to reside in the "zinc site" [17]. We have proposed that a tricopper cluster located at site D indeed is the catalytic site of pMMO. EPR and other biochemical data have provided strong evidence for the existence of this putative tricopper site, and the involvement of this site in the catalytic mechanism of the enzyme [1,16,38]. A tricopper-peptide complex has recently been prepared based on the PmoA peptide **H**IHA**M**LTMG**D**W**D** that lines the empty hydrophilic cavity at this site in the protein crystal structure of pMMO from *M. capsulatus* [16]. According to model building, the tricopper cluster is sequestered at site D by the ligands in bold in this peptide as well as an additional Glu from PmoA, together with another Glu from PmoC [38]. Upon activation of the $Cu^ICu^ICu^I$–peptide complex by dioxygen in the presence of propene or methane, rapid oxidation of these substrates has been observed at room temperature, with propene converted into propylene oxide and methane into methanol, respectively [16]. The same oxidation chemistry has also been demonstrated for a model inorganic complex consisting of a similar tricopper cluster [16]. So, if the oxidation of methane and other hydrocarbons by pMMO is indeed mediated by the putative tricopper cluster at site D in the enzyme, then the same model inorganic tricopper complex should be able to oxidize the suicide substrate HCCH to ketene (Scheme 2). Indeed, we find that this tricopper complex mediates facile oxidation of HCCH as well as CH_3CCH to yield highly reactive intermediates. The results of these experiments are presented in Section III of Supporting Information.

Recently, similar findings have been reported for ammonia monooxygenase (AMO) from *Nitrosomonas europaea*, the evolutionarily related ammonia oxidizer [39]. Here, as in pMMO, HCCH is a suicide substrate and it totally abolishes the AMO activity by forming one single chemical adduct with the enzyme. Based on MS-based analysis, it has been confirmed that HCCH is first oxidized to ketene, which then covalently modifies His 191 of the AmoA subunit. Since pMMO and AmoA are considered paralogs of each other, we conclude with a brief comparison of those features of the two enzymes that might bear on the mechanism of the HCCH inactivation. First, AMO also has a tricopper site with all the ligands at the site D conserved (Fig. S12). Second, the ligands for

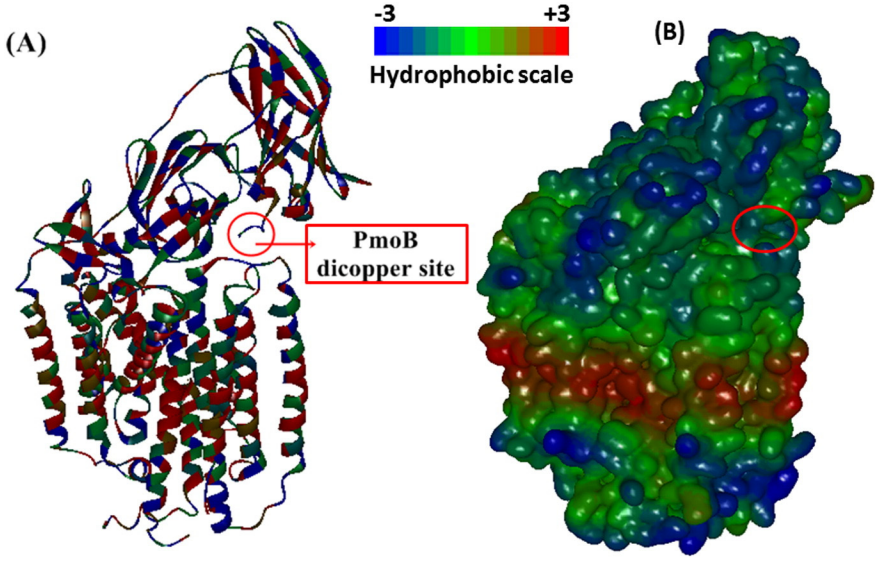

Fig. 6. (A) The hydrophobicity of the amino acid residues in pMMO. (B) The variation of the hydrophobicity of the protein surface of a pMMO monomer. The location of the PmoB dicopper site is highlighted. The site is clearly water-accessible.

the dicopper B site are also found in AMO, although they are not conserved in pMMO (Fig. S12). Third, in both cases, the enzyme is inhibited by acetylation at a single site, although the site of acetylation is different in the two enzymes, K196 of PmoC in the case of pMMO and H191 of AmoA in AMO. Interestingly, sequence alignments of the entire A and C subunits of the two enzymes (Fig. S13) show that these residues are not conserved, namely, H191 of AmoA is not found in PmoA and K196 of PmoC is not found in AmoC. Moreover, H191 is not associated with the putative tricopper cluster that has been designated as the catalytic site of the AMO. Thus, in the inhibition of the AMO, although the ketene is also formed by oxidation of the HCCH at the active site, it has migrated from this site to form a chemical adduct with a nucleophilic amino acid elsewhere as well. Given that the sequence similarities between the A and C subunits of the two enzymes are only ~40%, (44.6% between PmoA and AmoA, and 40.5% between PmoC and AmoC), we surmise that there must be substantial differences in the details of the protein folds between the two enzymes and in the ketene migration pathway(s) within the membranes of the two proteins, notwithstanding the different

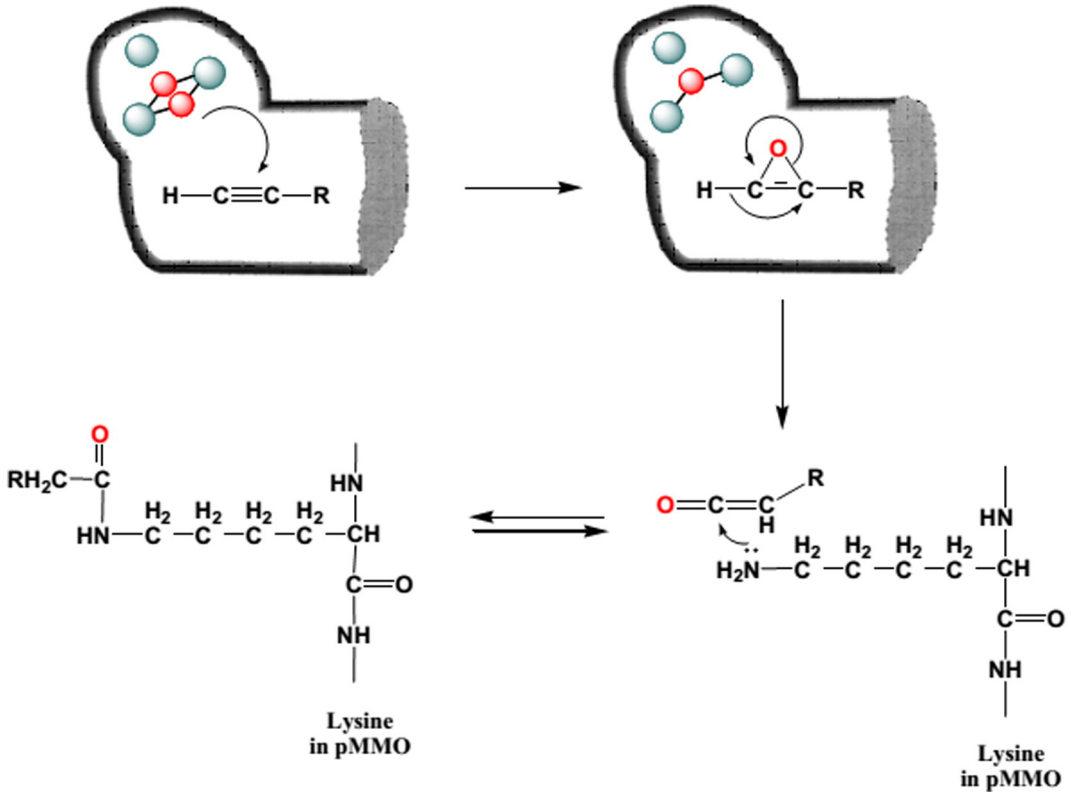

Scheme 2. A proposed mechanism for the formation of the ketene from oxidation of HCCH at the putative tricopper site of pMMO and the subsequent addition reaction of the ketene to the side chain (or acetylation) of a lysine residue.

locations of the nucleophilic amino acids available for acetylation in the two systems. Even in the case of pMMO, inhibitors with slightly different chemical structures, (*e.g.*, HCCH *vs* CH_3CCH), behave significantly differently in their patterns of chemical modification(s). In any case, it is hardly surprising, though intriguing, that the inactivation of AMO and pMMO by HCCH are so similar, that the reactive ketene is formed by oxidation of the HCCH by the conserved tricopper cluster site in the membrane, and acetylation of one amino acid within the transmembrane domain can rapidly abolish enzymatic activity in both cases.

The chemistry observed for the pMMO and AMO is also similar to the inactivation of keto steroid isomerase by an acetylene inhibitor, in which the keto steroid isomerase enzymatically converts acetylenic seco steroids into allenic ketones that alkylate the enzyme near the mouth of its active site [40].

Acknowledgment

We acknowledge numerous scientific discussions on this work with Dr. Chia-Min Yang (Department of Chemistry, National Tsing Hua University, Hsinchu, Taiwan). M.D. Pham is also grateful to Dr. Yang for serving as his academic advisor.

Appendix A. Supplementary data

Supplementary data to this article can be found online at http://dx.doi.org/10.1016/j.bbapap.2015.08.004.

References

[1] S.I. Chan, S.S.-F. Yu, Controlled oxidation of hydrocarbons by the membrane-bound methane monooxygenase: the case for a tricopper cluster, Acc. Chem. Res. 41 (2008) 969–979.
[2] S.J. Elliott, M. Zhu, L. Tso, H.-H.T. Nguyen, J.H.K. Yip, S.I. Chan, Regio- and stereoselectivity of particulate methane monooxygenase from *Methylococcus capsulatus* (Bath), J. Am. Chem. Soc. 119 (1997) 9949–9955.
[3] R.L. Lieberman, A.C. Rosenzweig, Biological methane oxidation: regulation, biochemistry, and active site structure of particulate methane monooxygenase, Crit. Rev. Biochem. Mol. Biol. 39 (2004) 147–164.
[4] B. Wilkinson, M. Zhu, N.D. Priestley, H.H.T. Nguyen, H. Morimoto, P.G. Williams, S.I. Chan, H.G. Floss, A concerted mechanism for ethane hydroxylation by the particulate methane monooxygenase from *Methylococcus capsulatus* (Bath), J. Am. Chem. Soc. 118 (1996) 921–922.
[5] M.A. Culpepper, A.C. Rosenzweig, Architecture and active site of particulate methane monooxygenase, Crit. Rev. Biochem. Mol. Biol. 47 (2012) 483–492.
[6] H.-H.T. Nguyen, S.J. Elliott, J.H.K. Yip, S.I. Chan, The particulate methane monooxygenase from *Methylococcus capsulatus* (Bath) is a novel copper-containing three-subunit enzyme — isolation and characterization, J. Biol. Chem. 273 (1998) 7957–7966.
[7] S.S.-F. Yu, K.H.-C. Chen, M.Y.-H. Tseng, Y.-S. Wang, C.-F. Tseng, Y.-J. Chen, D.-S. Huang, S.I. Chan, Production of high-quality particulate methane monooxygenase in high yields from *Methylococcus capsulatus* (Bath) with a hollow-fiber membrane bioreactor, J. Bacteriol. 185 (2003) 5915–5924.
[8] J.A. Zahn, A.A. DiSpirito, Membrane-associated methane monooxygenase from *Methylococcus capsulatus* (Bath), J. Bacteriol. 178 (1996) 1018–1029.
[9] D.W. Choi, R.C. Kunz, E.S. Boyd, J.D. Semrau, W.E. Antholine, J.I. Han, J.A. Zahn, J.M. Boyd, A.M. de la Mora, A.A. DiSpirito, The membrane-associated methane monooxygenase (pMMO) and pMMO-NADH : quinone oxidoreductase complex from *Methylococcus capsulatus* (Bath), J. Bacterial. 185 (2003) 5755–5764.
[10] R.L. Lieberman, A.C. Rosenzweig, Crystal structure of a membrane-bound metalloenzyme that catalyses the biological oxidation of methane, Nature 434 (2005) 177–182.
[11] A.S. Hakemian, K.C. Kondapalli, J. Telser, B.M. Hoffman, T.L. Stemmler, A.C. Rosenzweig, The metal centers of particulate methane monooxygenase from *Methylosinus trichosporium* OB3b, Biochemistry 47 (2008) 6793–6801.
[12] S.M. Smith, S. Rawat, J. Telser, B.M. Hoffman, T.L. Stemmler, A.C. Rosenzweig, Crystal structure and characterization of particulate methane monooxygenase from *Methylocystis* species strain M, Biochemistry 50 (2011) 10231–10240.
[13] S.I. Chan, H.-H.T. Nguyen, K.H.-C. Chen, S.S.-F. Yu, Overexpression and purification of the particulate methane monooxygenase from *Methylococcus capsulatus* (Bath), Methods Enzymol. 495 (2011) 177–193.
[14] R. Balasubramanian, S.M. Smith, S. Rawat, L.A. Yatsunyk, T.L. Stemmler, A.C. Rosenzweig, Oxidation of methane by a biological dicopper centre, Nature 465 (2010) 115–U131.
[15] S.I. Chan, K.H.-C. Chen, S.S.-F. Yu, C.-L. Chen, S.S.-J. Kuo, Toward delineating the structure and function of the particulate methane monooxygenase from methanotrophic bacteria, Biochemistry 43 (2004) 4421–4430.
[16] S.I. Chan, Y.-J. Lu, P. Nagababu, S. Maji, M.-C. Hung, M.M. Lee, I.-J. Hsu, M.D. Pham, J.C.-H. Lai, K.Y. Ng, S. Ramalingam, S.S.-F. Yu, M.K. Chan, Efficient oxidation of methane to methanol by dioxygen mediated by tricopper clusters, Angew. Chem. Int. Ed. 52 (2013) 3731–3735.
[17] M. Martinho, D.W. Choi, A.A. DiSpirito, W.E. Antholine, J.D. Semrau, E. Muenck, Mössbauer studies of the membrane-associated methane monooxygenase from *Methylococcus capsulatus* bath: evidence for a diiron center, J. Am. Chem. Soc. 129 (2007) 15783–15785.
[18] S.D. Prior, H. Dalton, Acetylene as a suicide substrate and active-site probe for methane monooxygenase from *Methylococcus capsulatus* (Bath), FEMS Microbiol. Lett. 29 (1985) 105–109.
[19] M.D. Pham, S.S.-F. Yu, C.-C. Han, S.I. Chan, Improved mass spectrometric analysis of membrane proteins based on rapid and versatile sample preparation on nanodiamond particles, Anal. Chem. 85 (2013) 6748–6755.
[20] A. Shevchenko, H. Tomas, J. Havlis, J.V. Olsen, M. Mann, In-gel digestion for mass spectrometric characterization of proteins and proteomes, Nat. Protoc. 1 (2006) 2856–2860.
[21] J. Polanska, M. Plechawska, M. Pietrowska, L. Marczak, Gaussian mixture decomposition in the analysis of MALDI-TOF spectra, Expert. Syst. 29 (2012) 216–231.
[22] M.P.a.P. Widłak, MALDI-MS-based profiling of serum proteome: detection of changes related to progression of cancer and response to anticancer treatment, Int. J. Proteomics 2012 (2012) 926427.
[23] J.C.G. Spainhour, M.G. Janech, J.H. Schwacke, J.C.Q. Velez, V. Ramakrishnan, The application of Gaussian mixture models for signal quantification in MALDI-ToF mass spectrometry of peptides, PLoS One 9 (2014) e111016.
[24] C.S.W. Zhang, W.S. Ross, D.A. Case, AmberTools Users' Manual, 2010.
[25] M.F. Sanner, Python: a programming language for software integration and development, J. Mol. Graphics Modell. 17 (1999) 57–61.
[26] O. Trott, A.J. Olson, Software news and update AutoDock Vina: improving the speed and accuracy of docking with a new scoring function, efficient optimization, and multithreading, J. Comput. Chem. 31 (2010) 455–461.
[27] D.F. Shanno, Conditioning of quasi-Newton methods for function minimization, Math. Comput. 24 (1970).
[28] D.H. Paull, A. Weatherwax, T. Lectka, Catalytic, asymmetric reactions of ketenes and ketene enolates, Tetrahedron 65 (2009) 6771–6803.
[29] T.T. Tidwell, Ketene chemistry after 100 years: ready for a new century, Eur. J. Org. Chem. 3 (2006) 563–576.
[30] V.M. Luna, J.A. Fee, A.A. Deniz, C.D. Stout, Mobility of Xe atoms within the oxygen diffusion channel of cytochrome ba(3) oxidase, Biochemistry 51 (2012) 4669–4676.
[31] S.J. Lee, M.S. McCormick, S.J. Lippard, U.-S. Cho, Control of substrate access to the active site in methane monooxygenase, Nature 494 (2013) 380–384.
[32] D.A. Whittington, A.C. Rosenzweig, C.A. Frederick, S.J. Lippard, Xenon and halogenated alkanes track putative substrate binding cavities in the soluble methane monooxygenase hydroxylase, Biochemistry 40 (2001) 3476–3482.
[33] N. Myronova, A. Kitmitto, R.F. Collins, A. Miyaji, H. Dalton, Three-dimensional structure determination of a protein supercomplex that oxidizes methane to formaldehyde in *Methylococcus capsulatus* (Bath), Biochemistry 45 (2006) 11905–11914.
[34] K.Y. Ng, L.-C. Tu, Y.-S. Wang, S.I. Chan, S.S.-F. Yu, Probing the hydrophobic pocket of the active site in the particulate methane monooxygenase (pMMO) from *Methylococcus capsulatus* (Bath) by variable stereoselective alkane hydroxylation and olefin epoxidation, Chembiochem 9 (2008) 1116–1123.
[35] A. Miyaji, T. Miyoshi, K. Motokura, T. Baba, The substrate binding cavity of particulate methane monooxygenase from *Methylosinus trichosporium* OB3b expresses high enantioselectivity for n-butane and n-pentane oxidation to 2-alcohol, Biotechnol. Lett. 33 (2011) 2241–2246.
[36] K.H.-C. Chen, C.-L. Chen, C.-F. Tseng, S.S.-F. Yu, S.-C. Ke, J.-F. Lee, H.-H.T. Nguyen, S.J. Elliott, J.O. Alben, S.I. Chan, The copper clusters in the particulate methane monooxygenase (pMMO) from *Methylococcus capsulatus* (Bath), J. Chin. Chem. Soc. 51 (2004) 1081–1098.
[37] W. Pritzkow, T.S.S. Rao, Studies on the autoxidation of phenylacetylene, J. Prakt. Chem. 327 (1985) 887–892.
[38] S.I. Chan, V.C.-C. Wang, J.C.-H. Lai, S.S.-F. Yu, P.P.-Y. Chen, K.H.-C. Chen, C.-L. Chen, M.K. Chan, Redox potentiometry studies of particulate methane monooxygenase: support for a trinuclear copper cluster active site, Angew. Chem. Int. Ed. 46 (2007) 1992–1994.
[39] S. Gilch, M. Vogel, M.W. Lorenz, O. Meyer, I. Schmidt, Interaction of the mechanism-based inactivator acetylene with ammonia monooxygenase of *Nitrosomonas europaea*, Microbiology-Sgm 155 (2009) 279–284.
[40] T.M. Penning, D.N. Heller, T.M. Balasubramanian, C.C. Fenselau, P. Talalay, Mass spectrometric studies of a modified active-site tetrapeptide from delta 5-3-ketosteroid isomerase of *Pseudomonas testosteroni*, J. Biol. Chem. 257 (1982) 12589–12593.